Infrared Spectroscopy of the Entrance Channel Complex Formed Between the Hydroxyl Radical and Methane in Helium Nanodroplets

Paul L. Raston[1], Emmanuel I. Obi[2], and Gary E. Douberly[2,*]

[1]*Department of Chemistry and Biochemistry, James Madison University, Harrisonburg, Virginia 22807, USA*

[2]*Department of Chemistry, University of Georgia, Athens, Georgia 30602, USA*

ABSTRACT

The entrance channel complex in the exothermic OH + CH_4 → H_2O + CH_3 reaction has been isolated in helium nanodroplets following the sequential pick-up of the hydroxyl radical and methane. The *a*-type OH stretching band was probed with infrared depletion spectroscopy, revealing a qualitatively similar spectrum to that previously reported in the gas phase, but with additional substructure that is due to the different internal rotation states of methane (j_{CH4} = 0, 1, or 2) in the complex. We fit the spectra by assuming the rotational constants of the complex are the same for all internal rotation states; however, subband origins are found to decrease with increasing j_{CH4}. Measurements of deuterated complexes have also been made (OD-CH_4, OH-CD_4, and OD-CD_4), the relative line widths of which provide information about the flow of vibrational energy in the complexes; vibrational lifetime broadening is prominent for OH-CH_4 and OD-CD_4 for which the excited OX stretching state has a nearby CY_4 stretching fundamental (X, Y = H or D).

*Corresponding Author: douberly@uga.edu; 01-706-542-3857

1. INTRODUCTION

Methane is the second strongest anthropogenic greenhouse gas on account of its relatively large mid-infrared (IR) cross section and rapidly rising atmospheric concentration, which has more than doubled since pre-industrial times.[1] It is primarily removed from Earth's atmosphere through the hydrogen-atom exchange reaction with the hydroxyl radical, which is also a significant sink for this "detergent of the atmosphere".[2] At much higher temperatures (~1000 K), this reaction is relevant to hydrocarbon combustion chemistry,[3] and at much lower temperatures (~10 K), it is suspected to play an important role in the eventual formation of complex organics in interstellar ices.[4] The entrance channel complex (OH-CH_4) has been characterized in cold (~3 K) molecular beam experiments, where its binding energy was determined to be only 210 cm^{-1},[5-7] and the floppy exit channel complex (CH_3-H_2O) has been investigated in even colder (0.4 K) helium nanodroplets, which allowed for the characterization of the loose hydrogen bonding nature of the intermolecular interaction.[8] Here, we uncover new dynamics in this system by investigating the entrance channel complex formed in helium nanodroplets from the association of OH and CH_4, and the various combinations of their perdeuterated isotopologues.

The OH-CH_4 complex has been investigated by IR action spectroscopy in both the OH[6] and CH[5, 7] stretching regions. In the OH stretching region, the band was consistent with that of a pseudodiatomic with unquenched hydroxyl radical electronic angular momentum, which is suggestive of a symmetric top structure having C_{3v} symmetry (see inset of Fig. 1). The peaks were too broad, however, to resolve the finer structure that was expected from the three nuclear spin isomers of methane (*A*, *F*, and *E*), which have differing values of their internal rotational angular momenta (j_{CH4} = 0, 1, or 2, in their ground states). The "splitting" was partially resolved (for the *A* and *F* species), however, in the broader symmetric CH stretching region. For the related CO-CH_4 complex, lines for all nuclear spin isomers of methane in the CO stretching region have been observed, but only the spectrum involving the *A* spin isomer of CH_4 was analyzed.[9] The CO-CH_4 complex has also been investigated by millimeter-wave spectroscopy, where lines from all three nuclear spin isomers have been analyzed.[10] Several other diatomic molecule-methane complexes have been investigated by microwave, IR, or electronic spectroscopy, including HCl-CH_4,[11-12] HF-CH_4,[12] HBr-CH_4,[13] H_2-CH_4,[14] and NO-CH_4.[15] Helium nanodroplet isolation provides a useful medium, which typically simplifies the spectroscopy, whilst allowing for rotational resolution for small to medium sized molecular systems.[16-18] Part of the motivation of this helium nanodroplet work is to resolve the three

sets of rovibrational peaks that originate from the free internal rotation states of methane in the weakly bound OX-CY_4 complex (X, Y = H or D).

The group of Lester also investigated the OD-CH_4 complex, for which the OD stretching overtone band was found to be significantly broader than for the analogous band in OH-CH_4.[19] This was attributed to vibrational lifetime effects, in that there are near resonances that lead to more efficient vibration-to-vibration (V-V) energy transfer in OD-CH_4. Similar evidences for intracomplex V-V energy transfer in helium nanodroplets have been reported for HF-CX_3[20] and HD-HF.[21] In the HD-HF complex, for example, a near resonance between the stretching fundamentals was invoked to (tentatively) explain the much broader lines in the HF stretching band than in H_2-HF and D_2-HF. In the IR spectra of the entrance channel complexes reported below (OH-CH_4, OH-CD_4, OD-CH_4, and OD-CD_4), we find convincing evidence for intracomplex V-V energy transfer (from OX to CY_4) from the differing linewidths between the sets of isotopologues. This bears relevance to understanding the reaction dynamics of this system, which have been investigated by crossed molecular beams,[22-24] where evidence for intracomplex V-V energy transfer has been found in the exit channel. Several recent theoretical investigations (e.g. Refs 25-28) have found good agreement with much of the crossed molecular beam data, in addition to the rate constant data over a broad temperature range (see Ref. 29 and those within).

2. EXPERIMENTAL

The hydroxyl (deuteroxyl) radicals were generated from the pyrolysis of tertbutyl hydroperoxide (deuteroperoxide) and doped into helium nanodroplets as previously described.[30, (31)] Following radical pick-up, methane or methane-d4 was doped into the droplets using a pick-up cell pressure that was optimized for, on average, one per droplet. The assembled complexes were then probed with the output of an Aculight OPO laser system that was tuned over a fairly narrow range,[32] due to the availability of previously reported gas phase spectra involving methane (OH-CH_4[5-7] and OD-CH_4[19]). Following IR photon absorption, the vibrationally hot complex decays through the evaporation of several hundred helium atoms. This decrease in droplet size is detected with a mass spectrometer, the signal from which is proportional to the droplet cross section. The mass spectrometer is equipped with a quadrupole ion guide that was used to mass select specific ion fragments. The selected mass fragments were H_3O^+ (m/z = 19 u) for OH-CH_4, H_2DO^+ (m/z = 20 u) for OD-CH_4, HD_2O^+ (m/z = 21 u) for OH-CD_4, and D_3O^+ (m/z = 22 u) for OD-CD_4. The mass specific

spectra are inverted so that a positive peak corresponds to a laser-induced reduction in the ionization cross section of the droplet beam. The interested reader is referred elsewhere for further experimental details.[18, 32-34]

3. RESULTS AND DISCUSSION

Spectra and Assignments

i. Normal isotopologue (OH-CH_4)

The OH stretching fundamental band of the OH-CH_4 complex was previously investigated in the gas phase via IR action spectroscopy, from which the band origin was determined to be 3563.45 cm^{-1}.[6] Since vibrational shifts in going from the gas phase to helium nanodroplets are on the order of 1 cm^{-1},[35] we did not have to search far before observing depletion signal corresponding to the analogous band in helium nanodroplets (Fig. 1). The mass selected signal was relatively weak on account of the large distribution in the masses of ions produced following the electron impact ionization of OH-CH_4 doped droplets (see Fig. S1), and so significant averaging was required to obtain good S/N. We used mass channel 19 u when recording spectra because it gave slightly better S/N than other candidate channels, whilst retaining good selectivity against "background" signals.

The spectrum consists of more lines than expected for a simple pseudodiatomic on account of the three different values of the internal rotational angular momentum of CH_4, which is directed along the principal axis of the complex (see inset of Fig. 1); this gives rise to three different subbands. The *Q* branch peak for each subband was found to saturate at relatively low power, as can be discerned from the power dependent spectra in Fig. 1. At high power, we detected peaks from weakly populated states not apparent at low power, but this was at the expense of power broadening, which resulted in complete blending of two *Q* branch peaks (*E* and *F* species) that are "well" resolved in the low power spectrum (which has ~2x narrower linewidths). All three expected *Q* branch peaks were observed for the regular isotopologue, which are labelled by the nuclear spin species of methane in the complex (Fig. 1). The assignment is supported by the intensity ratio between the peaks, which was determined to be 5:9:1.4, which compares reasonably well with the expected 5:9:2 ratio for the *A*, *F*, and *E* spin species (see Fig. S2).

The *P* and *R* branches begin at a separation of ~5*B* relative to the *Q* branch peaks, with some degree of convolution between the *P* and *R* branch peaks between the different internal

rotation states of methane in the complex. This spacing is most obvious for the more abundant *F* species, and is indicative of unquenched half integer orbital angular momentum in the complex. Naturally, this comes from the OH moiety, which does not seem to experience enough of an anisotropy in the intermolecular potential that would otherwise partially orient the electronic angular momentum in the *b*-*c* plane (perpendicular to the intermolecular axis); such partial quenching has been observed in helium nanodroplets for other complexes, such as OH-C_2H_2[36] and OH-H_2O,[37] but not for the related (linear) OH-CO complex.[38]

The type of fit we perform here is based on the gas phase study, where the orbital and spin angular momentum of OH (L = 1 and S = 1/2, respectively) was found to be fully projected onto the intermolecular axis. We therefore set this projection (usually labelled P) to be 3/2 in the ground and excited vibrational states, and fit the spectrum using an effective Hamiltonian appropriate for an open shell pseudo-diatomic conforming to Hund's case (a), with the computer program, PGOPHER.[39] The following equation was used for the transition frequencies:

$$\Delta E = \nu_{j_{\mathrm{CH4}}} + B'[J'(J'+1) - 3/4] - B''[J''(J''+1) - 3/4]$$
$$- \overline{D}_J[((J'(J'+1))^2 - 1/2J'(J'+1) - 3/16) - ((J''(J''+1))^2 - 1/2J''(J''+1) - 3/16)]$$

Here, we assume that the B rotational constants are independent of j_{CH4}, and that D is the same in the ground and excited vibrational states, which have band origins, $\nu_{j_{\mathrm{CH4}}}$. For simplicity we use the nuclear spin symmetry species of methane in place of j_{CH4}, i.e. ν_A, ν_F, and ν_E for j_{CH4} = 0, 1, and 2, respectively. The resulting parameters from the fit are listed in Table 1, where they are compared with the gas phase values. As expected, the vibrational shift is very small (see section 3.Vibrational Dynamics.*i.*), and the B rotational constant is reduced to 0.42x its gas phase value due to the coupling of helium density to molecular rotation.[35]

It is worth noting that we attempted to measure the *b*-type spectrum of OH-CH_4 and OD-CH_4 in the 3000-3040 cm^{-1} CH_4 stretching region (m/z = 19 u and partially on 20 u, respectively), however, it was very difficult to separate features due to other impurity species in the beam, such as the acetone-methane complex, and so we decided to not pursue this further.

ii. Minor isotopologues (OD-CH_4, OH-CD_4, and OD-CD_4)

We begin this subsection with an analysis of the OD stretching band of OD-CH_4, which has the sharpest, most highly resolved peaks. It was found ~1 cm^{-1} to the red of the predicted value of 2626.6 cm^{-1}, which was made by scaling the analogous shift in the non-deuterated complex *viz*, $\Delta\nu_{OD} = \Delta\nu_{OH} \times \nu_{OD}/\nu_{OH}$. Its spectrum is shown in Fig. 2, where we have labelled individual transitions to peaks for the *F* species. The OX stretching bands of the other two minor isotopologues, i.e. OH-CD_4 (Fig. 3), and OD-CD_4 (Fig. 4) were found <0.1 cm^{-1} from the respective OH-CH_4, and OD-CH_4 bands. The ~5*B* spacing between the central *Q* branch and neighboring *P*/*R* branch lines is evident for all minor isotopologues of the complex investigated, once again indicating that the spin-orbital angular momentum of the deuteroxyl/hydroxyl radical in the complex is unquenched (i.e. $P \approx 3/2$). As with the other normal isotopologue, we recorded the OX stretching spectra of the minor isotopologues at low power (<100 mW) to minimize saturation broadening.

The spectroscopic parameters of the minor isotopologues, along with further details of the fits are provided in Table 1, and a comparison of all four spectra is shown in Fig. S3. For all isotopologues, the subband origin decreases in going from ν_A to ν_F to ν_E. The finding that the subband origin shifts to lower wavenumber with increasing j_{CH4}, suggests that the internal rotation constant, b_J, is lower in the vibrationally excited state than in the ground state. We suspect this is due to the larger dipole moment of OH in v=1, which results in a greater anisotropy of the intermolecular potential. To model this effect, we would need to perform a detailed analysis similar to what has been suggested by Ohshima and Endo for the related HCl-CH_4 system.[11] Note that the subband origins for perdeuterated methane containing complexes are much closer together, which is due to the smaller internal rotational constant of CD_4; while we do not resolve different nuclear spin isomers in the fully deuterated complex (Fig. 4), we do observe evidence for all three in OH-CD_4 (Fig. 3). One of the most interesting aspects of this work is that the linewidths between the different isotopologues varies by up to 3x, and this is discussed below (section 3.Vibrational Dynamics.*ii*.).

Vibrational Dynamics

i. Normal isotopologue

The gas to helium droplet band origin shift amounts to ~1.3 cm^{-1}, which corresponds to the difference between the gas phase average band origin (over the 3 nuclear spin species of methane),[6] and the helium droplet *F* species subband origin. The (blended) homogeneous linewidth observed in the gas phase study was 0.14(2) cm^{-1}, with the dominant source of instrumental broadening coming from the IR pump laser, having a bandwidth of 0.04 cm^{-1}. Coincidentally, this is about the same as the linewidths observed here in the OH stretching band (in the low power spectrum), and so if the splitting between the subbands (labelled by the nuclear spin species of methane, i.e. *E*, *F*, and *A*) is the same in both environments (gas phase and helium nanodroplets), then the gas phase spectra in the absence of lifetime or power broadening effects should look similar in the *Q* branch region.

The vibrational lifetime of OH-CH_4 was given as an upper limit in the gas phase, since it was determined by linearly extrapolating a plot of signal intensity against laser power to zero power (which should be non-linear at low power).[6] Unfortunately this does not allow for one to separate lifetime from power broadening effects. If lifetime broadening dominates the linewidth in the gas phase, then the vibrational lifetime is much longer in helium nanodroplets (as evidenced by the narrower linewidths), which is in contrast to the effect that helium has on the vibrational lifetime of complexes studied so far; e.g. the HCN dimer[40] and the HF dimer[41] have shorter vibrational lifetimes in helium nanodroplets. We note, however, that the factor of 2 decrease in Lorentzian linewidths in going from the gas phase to helium nanodroplets for OH-CH_4 is similar to what was reported for HOOO (Γ = 0.212(8) cm^{-1} in the gas phase[42] and Γ = 0.1 cm^{-1} in helium nanodroplets[34]), and it was stated in the gas-phase study that the corresponding spectrum was not power broadened (as deduced from the linewidth not changing with laser power).[42] If we assume that for OH-CH_4, the dominant source of gas phase broadening is from near resonant V-V energy transfer,[6, 19] then we are left with the counterintuitive conclusion that the rate of transfer is slower in helium nanodroplets. On the basis of the aforementioned previous studies, in which vibrational lifetimes are reduced for the helium-solvated systems, we conclude instead that power broadening effects are responsible for the ~2x broader lines in the gas phase measurement.

ii. Minor isotopologues

Out of the minor isotopologue containing complexes investigated here, only OD-CH_4 has been investigated in the gas phase. Its OD stretching overtone spectrum was reported,[19] which can be directly compared to the OH stretching overtone spectrum for the normal isotopologue.[6] The comparison shows that there is a large reduction in the linewidth in the gas phase in going from OH [0.21(2) cm^{-1}][6] to OD [0.10(1) cm^{-1}].[19] The faster decay of the excited state for OH-CH_4 was broadly attributed to prereaction and/or predissociation. Analysis of the rotational energy distribution of the predissociated OX radicals more specifically indicated that near resonant V-V transfer is responsible for the faster decay in OH-CH_4 compared to OD-CH_4.[19] In helium nanodroplets we see a similar reduction in the linewidths in going from OH [0.035(5) cm^{-1}] to OD [0.013(3) cm^{-1}].

Fig. 5 shows a comparison of the linewidths in the *Q* branch region for all isotopologues of the complex under investigation, along with an energy level diagram which plots the potential V-V relaxation channels. For the normal isotopologue, the OH stretch can decay to one quanta of CH stretch, leaving behind ~550 cm^{-1} excess energy, which must be redistributed to other molecular/droplet collective degrees of freedom. In comparison, the OD stretch can decay to one quanta of CH_4 bend, requiring the redistribution of twice the excess energy as for OH (~1100 cm^{-1}). This suggests that the narrower (broader) lines in the OD (OH) stretching fundamentals result from a larger (smaller) energy gap between the excited state and nearest accessible relaxation channel, i.e. the difference in lifetimes is due to faster V-V transfer in OH-CH_4, which is similar to what was observed in the gas phase overtone spectra.[6, 19]

Upon switching the methane partner to perdeuterated methane, we switch the energy gaps so that the excited OH(D)-CD_4 complex now has a very large (small) amount of excess energy upon V-V relaxation (Fig. 5). This is reflected in the linewidths, for which OH-CD_4 is about as narrow as OD-CH_4, while OD-CD_4 is about as broad as OH-CH_4. We note that the energy difference between the fundamental of OH and the overtone of the CD_4 bend is similar to that between the OH and CH_4 stretching fundamentals. Nevertheless the OH stretch line widths are similar to those for OD-CH_4. This likely reflects the comparatively poorer coupling of the OH v=1 stretching state to overtone/combination CD_4 bending states.

4. SUMMARY

We report the *a*-type IR spectrum (OX stretch where X=H/D) of the van der Waals complex formed between the hydroxyl radical and methane in helium nanodroplets. The spectra in the OH and OD stretching regions consist of the convolution of three subbands that originate from the different internal rotation ground states of methane (j_{CH4} = 0, 1, and 2, for the *A*, *F*, and *E* spin species, respectively). The subbands were largely resolved for OX-CH_4 and unresolved for OX-CD_4, for which the splitting due to the heavier methane was much smaller. The decrease in subband origin with increasing j_{CH4} indicates a reduction in the internal rotation constant upon OX stretch vibrational excitation, which is consistent with the larger dipole moment of OX in the excited vibrational state and the expected increase in the intermolecular anisotropy. From the spacing between the *P*, *Q*, and *R* branch peaks in the helium droplet spectra, it is apparent that the internal rotational anisotropy experienced by the singly occupied pπ orbital in the *b*/*c* plane is too weak to induce any localizing effects, i.e. the spin-orbit angular momentum is in the unquenched limit, which is the same as what was determined from lower resolution gas phase spectra.[6, 19] Comparison of the linewidths between the different isotopologic complexes indicates that resonant V-V transfer dominates the linewidths for the species with smaller energy gaps between the excited OX stretching state and next lowest in energy methane fundamental vibrational state.

Supporting Information

Difference mass spectrum for OH stretching band of OH-CH_4; Lorentzian fits to the OD-CH_4 *Q*-branch peaks; Comparison of all four spectra in the OX stretching regions.

ACKNOWLEDGEMENTS

G.E.D acknowledges support from the Office of Energy Research, Office of Basic Energy Sciences, Chemical Sciences, Geosciences and Biosciences Division of the US Department of Energy (DOE) under Contract No. DE-FG02-12ER16298.

Table 1. Ground and excited OX stretching state rotational constant, average centrifugal distortion constant, and methane nuclear spin species subband origins for OX-CY$_4$ embedded in helium nanodroplets.

	OH-CH$_4$		OD-CH$_4$		OH-CD$_4$	OD-CD$_4$
constant	gas phase[a]	He droplet	gas phase[b]	He droplet	He droplet	He droplet
B''	0.15(1)	0.0627(8)	0.144(1)	0.0618(6)	0.0591(2)	0.0584(5)
B'	0.15(1)	0.0625[c]	-	0.0616(7)	0.0588(6)	0.0578(8)
$\overline{D}_J$	-	0.00017[d]	-	0.00017(3)	0.00017(3)	0.00017[e]
ν_E	-	3562.024(6)	-	2625.516(1)	3562.073[f]	2625.599[f]
ν_F	3563.45(5)[g]	3562.084(3)	-	2625.557(1)	3562.087(2)	2625.606(3)
ν_A	-	3562.177(3)	-	2625.621(1)	3562.110(2)	2625.619[f]
Γ[h]	0.14(2)	0.035(5)	-	0.013(3)	0.016(3)	0.030(5)

[a]Ground state constant from Ref 6.

[b]Ground state constant from Ref 19.

[c]Difference between B' and B'' fixed to value for OD-CH$_4$.

[d]Fixed to value for OD-CH$_4$.

[e]Fixed to value for OH-CD$_4$.

[f]Assumed scaled value

[g]Central unresolved Q branch peak.

[h]Full-width at half-maximum linewidth.

REFERENCES

1. *IPCC (2013) Climate Change 2013: The Physical Science Basis. Contribution of Working Group I to the Fifth Assessment Report of the Intergovernmental Panel on Climate Change, Eds Stocker Tf, Qin D, Plattner G-K, Tignor M, Allen Sk, Boschung J, Nauels a, Xia Y, Bex V, Midgley Pm (Cambridge Univ Press, Cambridge, UK).*

2. Naik, V.; Voulgarakis, A.; Fiore, A. M.; Horowitz, L. W.; Lamarque, J. F.; Lin, M.; Prather, M. J.; Young, P. J.; Bergmann, D.; Cameron-Smith, P. J.; et.al., Lifetime from the Atmospheric Chemistry and Climate Model Intercomparison Project (ACCMIP) *Atmos. Chem. Phys.* **2013,** *13*, 5277-5298.

3. Glassman, I. *Combustion, 3rd Ed.*; Academic Press: San Diego, Califonia, 1996.

4. Lamberts, T.; Fedoseev, G.; Kästner, J.; Ioppolo, S.; Linnartz, H., Importance of Tunneling in H-Abstraction Reactions by OH Radicals *Astron. Astrophys.* **2017,** *599*, A132.

5. Tsiouris, M.; Wheeler, M. D.; Lester, M. I., Stimulated Raman and Electronic Excitation of CH_4-OH Reactant Complexes *Chem. Phys. Lett.* **1999,** *302*, 192-198.

6. Wheeler, M. D.; Tsiouris, M.; Lester, M. I.; Lendvay, G., OO Vibrational Activation and Decay Dynamics of CH_4-OH Entrance Channel Complexes *J. Chem. Phys.* **2000,** *112*, 6590-6602.

7. Tsiouris, M.; Wheeler, M. D.; Lester, M. I., Activation of the CH Stretching Vibrations in CH_4-OH Entrance Channel Complexes: Spectroscopy and Dynamics *J. Chem. Phys.* **2001,** *114*, 187-197.

8. Rudic, S.; Merritt, J. M.; Miller, R. E., Study of the CH_3-H_2O Radical Complex Stabilized in Helium Nanodroplets *Phys. Chem. Chem. Phys.* **2009,** *11*, 5345-5352.

9. Xia, C. H.; Walker, K. A.; McKellar, A. R. W., Infrared and Millimeter Wave Spectra of the CH_4-CO Complex in the a Internal Rotation State *J. Chem. Phys.* **2001,** *114*, 4824-4828.

10. Surin, L. A.; Tarabukin, I. V.; Panfilov, V. A.; Schlemmer, S.; Kalugina, Y. N.; Faure, A.; Rist, C.; van der Avoird, A., Rotational Study of the CH_4-CO Complex: Millimeter-Wave Measurements and Ab Initio Calculations *J. Chem. Phys.* **2015,** *143*, 154303.

11. Ohshima, Y.; Endo, Y., Rotational Spectrum and Internal Rotation of a Methane–HCl Complex *J. Chem. Phys.* **1990,** *93*, 6256-6265.

12. Legon, A. C.; Roberts, B. P.; Wallwork, A. L., Rotational Spectra and Geometries of the Gas-Phase Dimers (CH_4,HF) and (CH_4,HCl) *Chem. Phys. Lett.* **1990,** *173*, 107-114.

13. Atkins, M. J.; Legon, A. C.; Wallwork, A. L., The Pairwise Interaction of Methane and Hydrogen Bromide: Properties of the Weakly Bound Dimer CH_4-HBr from Microwave Spectroscopy *Chem. Phys. Lett.* **1992,** *192*, 368-374.

14. McKellar, A. R. W.; Roth, D. A.; Pak, I.; Winnewisser, G., The Weakly Bound Complex CH_4-H_2: Observation and Analysis of Infrared Spectra in the 350 and 1311 cm^{-1} Regions *J. Chem. Phys.* **1999,** *110*, 9989-9996.

15. Daire, S. E.; Lozeille, J.; Gamblin, S. D.; Wright, T. G.; Lee, E. P. F., The $\tilde{A}^2\Sigma^+ \leftarrow X^2\Pi$ Transition of the NO-CH_4 and NO-CD_4 Complexes *Phys. Chem. Chem. Phys.* **2001,** *3*, 917-924.

16. Toennies, J. P.; Vilesov, A. F., Superfluid Helium Droplets: A Uniquely Cold Nanomatrix for Molecules and Molecular Complexes *Angew. Chem. Int. Ed.* **2004,** *43*, 2622-2648.

17. Stienkemeier, F.; Lehmann, K. K., Spectroscopy and Dynamics in Helium Nanodroplets *J. Phys. B At. Mol. Cl.* **2006,** *39*, R127-R166.

18. Choi, M. Y.; Douberly, G. E.; Falconer, T. M.; Lewis, W. K.; Lindsay, C. M.; Merritt, J. M.; Stiles, P. L.; Miller, R. E., Infrared Spectroscopy of Helium Nanodroplets: Novel Methods for Physics and Chemistry *Int. Rev. Phys. Chem.* **2006,** *25*, 15-75.

19. Tsiouris, M.; Pollack, I. B.; Lester, M. I., Infrared Action Spectroscopy and Inelastic Recoil Dynamics of the CH_4-OD Reactant Complex *J. Phys. Chem. A* **2002,** *106*, 7722-7727.

20. Merritt, J. M.; Rudic, S.; Miller, R. E., Infrared Laser Spectroscopy of CH_3-HF in Helium Nanodroplets: The Exit-Channel Complex of the F+CH_4 Reaction *J. Chem. Phys.* **2006,** *124*, 084301.

21. Moore, D. T.; Miller, R. E., Dynamics of Hydrogen-HF Complexes in Helium Nanodroplets *J. Chem. Phys.* **2003,** *118*, 9629-9636.

22. Zhang, B. L.; Shiu, W. C.; Lin, J. J.; Liu, K. P., Mode Correlation of Product Pairs in the Reaction OH+CD_4 -> HOD+CD_3 *J. Chem. Phys.* **2005,** *122*, 131102.

23. Zhang, B. L.; Shiu, W. C.; Liu, K., Imaging the Reaction Dynamics of OH+CD_4. 2. Translational Energy Dependencies *J. Phys. Chem. A* **2005,** *109*, 8983-8988.

24. Zhang, B. L.; Shiu, W. C.; Liu, K., Imaging the Reaction Dynamics of OH+CD_4. 3. Isotope Effects *J. Phys. Chem. A* **2005,** *109*, 8989-8993.

25. Song, H. W.; Lee, S. Y.; Yang, M. H.; Lu, Y. P., Six-Dimensional and Seven-Dimensional Quantum Dynamics Study of the OH + $CH_4 \rightarrow H_2O$ + CH_3 Reaction *J. Chem. Phys.* **2013,** *139*, 154310.

26. Song, H. W.; Li, J.; Jiang, B.; Yang, M. H.; Lu, Y. P.; Guo, H., Effects of Reactant Rotation on the Dynamics of the OH + $CH_4 \rightarrow H_2O + CH_3$ Reaction: A Six-Dimensional Study *J. Chem. Phys.* **2014,** *140*, 084307.

27. Espinosa-Garcia, J.; Corchado, J. C., QCT Dynamics Study of the Reaction of Hydroxyl Radical and Methane Using a New Ab Initio Fitted Full-Dimensional Analytical Potential Energy Surface *Theor. Chem. Acc.* **2015,** *134*, 6.

28. Li, J.; Guo, H., Communication: An Accurate Full 15 Dimensional Permutationally Invariant Potential Energy Surface for the OH + $CH_4 \rightarrow H_2O + CH_3$ Reaction *J. Chem. Phys.* **2015,** *143*, 221103.

29. Srinivasan, N. K.; Su, M. C.; Sutherland, J. W.; Michael, J. V., Reflected Shock Tube Studies of High-Temperature Rate Constants for OH + $CH_4 \rightarrow CH_3$+ H_2O and CH_3+$NO_2 \rightarrow$ CH_3O+NO *J. Phys. Chem. A* **2005,** *109*, 1857-1863.

30. Raston, P. L.; Liang, T.; Douberly, G. E., Anomalous Lambda-Doubling in the Infrared Spectrum of the Hydroxyl Radical in Helium Nanodroplets *J. Phys. Chem. A* **2013,** *117*, 8103-8110.

31. Raston, P. L.; Liang, T.; Douberly, G. E., Observation of the Q(3/2) Lambda-Doublet Transitions for $X^2\Pi_{3/2}$ OD in Helium Nanodroplets *Mol. Phys.* **2014,** *112*, 301-303.

32. Morrison, A. M.; Liang, T.; Douberly, G. E., Automation of an "Aculight" Continuous-Wave Optical Parametric Oscillator *Rev. Sci. Inst.* **2013,** *84*, 013102.

33. Morrison, A. M.; Flynn, S. D.; Liang, T.; Douberly, G. E., Infrared Spectroscopy of $(HCl)_M(H_2O)$+ Clusters in Helium Nanodroplets: Definitive Assignments in the HCl Stretch Region *J. Phys. Chem. A* **2010,** *114*, 8090-8098.

34. Raston, P. L.; Liang, T.; Douberly, G. E., Infrared Spectroscopy of HOOO and DOOO in He-4 Nanodroplets *J. Chem. Phys.* **2012,** *137*, 184302.

35. Callegari, C.; Lehmann, K. K.; Schmied, R.; Scoles, G., Helium Nanodroplet Isolation Rovibrational Spectroscopy: Methods and Recent Results *J. Chem. Phys.* **2001,** *115*, 10090-10110.

36. Douberly, G. E.; Raston, P. L.; Liang, T.; Marshall, M. D., Infrared Rovibrational Spectroscopy of OH-C_2H_2 in He-4 Nanodroplets: Parity Splitting Due to Partially Quenched Electronic Angular Momentum *J. Chem. Phys.* **2015,** *142*, 134306.

37. Hernandez, F. J.; Brice, J. T.; Leavitt, C. M.; Liang, T.; Raston, P. L.; Pino, G. A.; Douberly, G. E., Mid-Infrared Signatures of Hydroxyl Containing Water Clusters: Infrared Laser Stark Spectroscopy of OH-H_2O and $OH(D_2O)_N$ (N=1-3) *J. Chem. Phys.* **2015,** *143*, 164304.

38. Brice, J. T.; Liang, T.; Raston, P. L.; McCoy, A. B.; Douberly, G. E., Infrared Stark and Zeeman Spectroscopy of OH-CO: The Entrance Channel Complex Along the OH + CO → Trans-HOCO Reaction Pathway *J. Chem. Phys.* **2016,** *145*, 124310.

39. Western, C. M., Pgopher: A Program for Simulating Rotational, Vibrational and Electronic Spectra *J. Quant. Spectros. Radiat. Transfer* **2017,** *186*, 221-242.

40. Nauta, K.; Miller, R. E., Solvent Mediated Vibrational Relaxation: Superfluid Helium Droplet Spectroscopy of HCN Dimer *J. Chem. Phys.* **1999,** *111*, 3426-3433.

41. Nauta, K.; Miller, R. E., The Hydrogen Fluoride Dimer in Liquid Helium: A Prototype System for Studying Solvent Effects on Hydrogen Bonding *J. Chem. Phys.* **2000,** *113*, 10158-10168.

42. Derro, E. L.; Murray, C.; Sechler, T. D.; Lester, M. I., Infrared Action Spectroscopy and Dissociation Dynamics of the HOOO Radical *J. Phys. Chem. A* **2007,** *111*, 11592-11601.

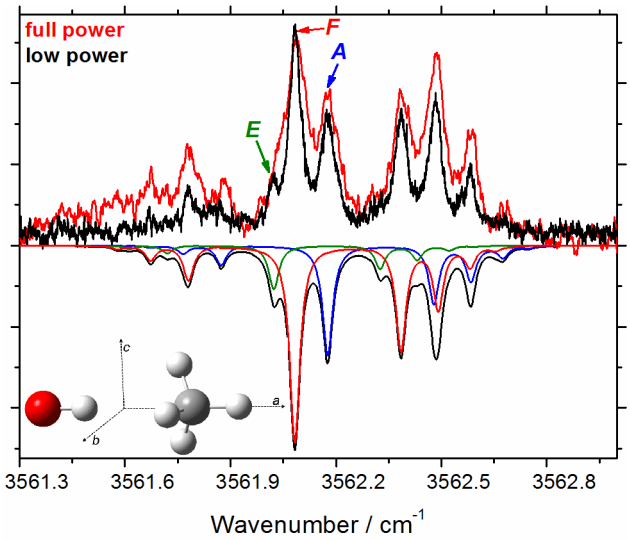

Fig. 1. High and low power scans of OH-CH_4 in helium nanodroplets, shown in red and black, respectively. Inverted spectra are simulations using parameters listed in Table 1 and a temperature of 0.4 K, where green corresponds to the *E* nuclear spin species of methane (*J*=2), red is *F* (*J*=1), and blue is *A* (*J*=0). The average structure taken from Ref. [6] is also shown.

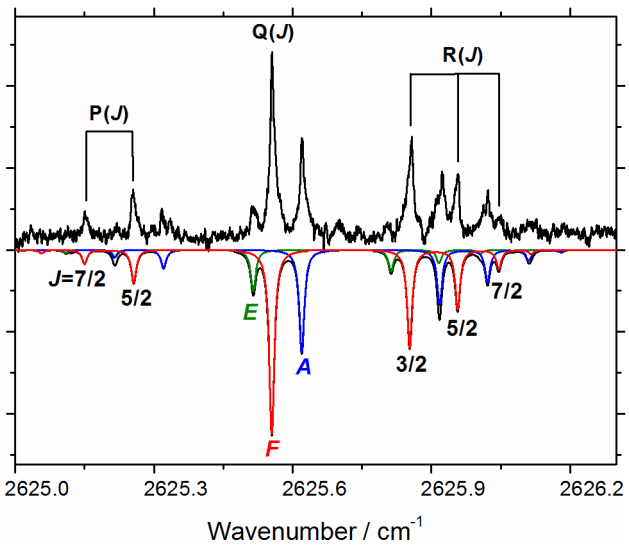

Fig. 2. Spectrum and simulation of OD-CH_4 in helium nanodroplets using parameters listed in Table 1. Transitions corresponding to the *F* species (red) methane are labelled.

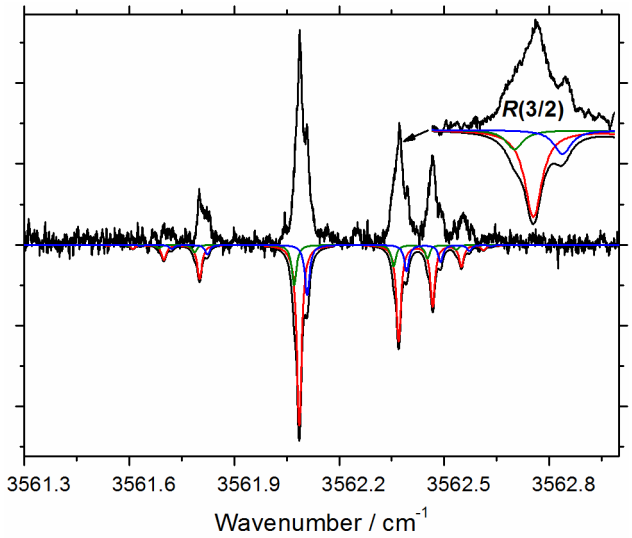

Fig. 3. Spectrum and simulation of OH-CD_4 in helium nanodroplets using parameters listed in Table 1. The expected 5:18:4 ratio for the *A* (blue), *F* (red), and *E* (green) spin species of CD_4 are used to weight the relative intensities of the subbands. Note the weak hump on the red edge of the *R*(3/2) peak, which is likely due to the *E* species complex.

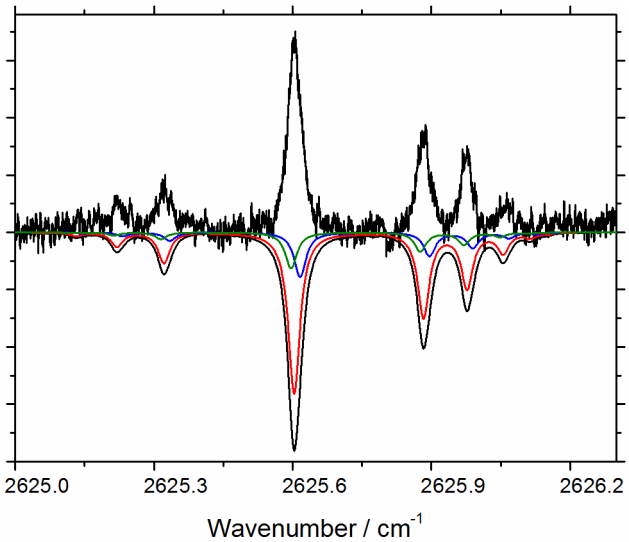

Fig. 4. Spectrum and simulation of OD-CD_4 in helium nanodroplets using parameters listed in Table 1. The expected 5:18:4 ratio for the *A* (blue), *F* (red), and *E* (green) spin species of CD_4 are used to weight the relative intensities of the subbands.

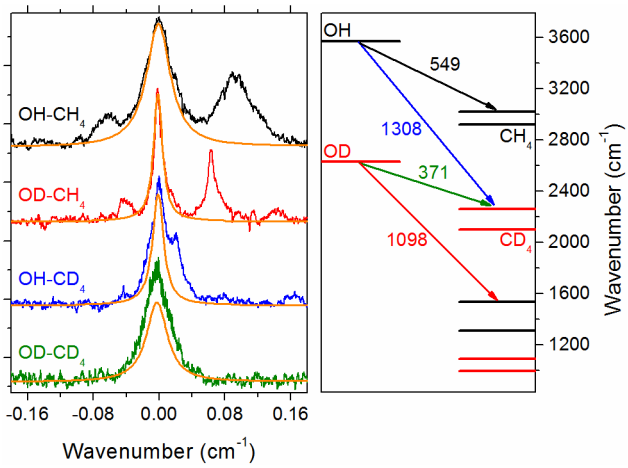

Fig. 5. Left: Comparison of OX stretching *Q* branches and fitted Lorentzians for *F* species peak (orange). Right: Energy level diagram showing OX and CY_4 fundamental modes and lowest energy relaxation channels between them for each complex.
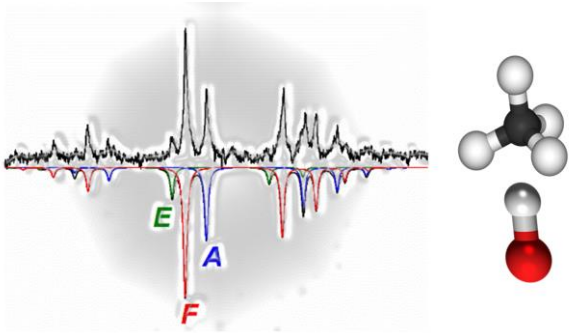
TOC GRAPHIC